Magnetic Properties and Crystalline Fields in $YbPd_3$†

I. Nowik,* B. D. Dunlap, and G. M. Kalvius‡
Argonne National Laboratory, Argonne, Illinois 60439
(Received 22 February 1972)

Mössbauer-effect studies of ^{170}Yb in the cubic intermetallic $YbPd_3$ at temperatures 1.4–4.2 K and in external fields up to 44 kOe yield the following results: (a) Although the Yb ion is trivalent, no magnetic ordering is seen down to 1.4 K. (b) The temperature and field dependence of the magnetic hyperfine field and the induced electric field gradient show that the ground state in the presence of external field is not an isolated level. (c) All experimental observations can be reproduced by a cubic-crystalline-field calculation with parameters $A_4\langle r^4\rangle = -12 \pm 1$ cm^{-1} and $A_6\langle r^6\rangle = 0.6 \pm 0.6$ cm^{-1}. These give a Γ_7 ground state with Γ_8 and Γ_6 lying at 29 and 39 cm^{-1}. These results are compared to predictions of a simple-point-charge-model calculation. Low-field spectra have been analyzed to give an ionic-spin-relaxation time $\tau_R \simeq 4 \times 10^{-11}$ sec.

INTRODUCTION

The magnetic properties of rare earths in insulators are well understood in terms of crystalline field theory. The effect of crystalline fields on the properties of rare earths in metallic systems is much less understood, largely because our principal sources of information on crystal field parameters (electron-spin resonance and optical spectroscopy) are very difficult in metals. In recent years some information has become available through the use of neutron diffraction,[1] susceptibility measurements,[2] specific heat, Mössbauer-effect studies, and some ESR work.[3] Most of this work has involved cubic systems since in this case only two parameters are required to discuss the experimental results, i.e., the crystal field parameters $A_4\langle r^4\rangle$ and $A_6\langle r^6\rangle$. In general, one finds that, in contrast to insulators, crystal fields for metals are rather small. This is generally discussed in terms of shielding effects on the ions of the crystal by the conduction electrons.

In order to obtain more information on the subject, it is useful to study single-electron or single-hole ions, such as $Ce^{3+}(4f^1)$ or $Yb^{3+}(4f^{13})$. From a theoretical point of view these may be easily treated within the crystal field approximation, with a minimum of calculational difficulty. Experimentally, measurements of hyperfine interactions such as one obtains, for example, in the Mössbauer effect are very useful because they provide a truly local measure of the ion's behavior. If external magnetic fields can be applied which are sufficiently large to cause admixtures of the crystal field levels, then the resulting hyperfine constants in principle can be analyzed to provide a complete discussion of the crystal field effects. Here we present a detailed study of the crystalline fields acting on Yb^{3+} in $YbPd_3$, which has the face-centered-cubic Cu_3Au structure.[4] The crystalline field parameters have been obtained by a study of the dependence of the hyperfine interaction in ^{170}Yb, as measured by the Mössbauer effect, on temperature and external field.

EXPERIMENTAL

Data were obtained with the Mössbauer effect of the 84.3-keV resonance in ^{170}Yb. The source material was ^{170}Tm in a $TmAl_2$ matrix. Absorbers were unenriched $YbPd_3$ with a total material thickness of 300 mg/cm^2. Both source and absorber were placed in a superconducting magnet with the magnetic field along the direction of γ-ray propagation. External fields up to 44 kOe were applied at temperatures of 4.2 and 1.4 K.

The 84.3-keV γ ray in ^{170}Yb results from an $E2$ transition between an excited-state spin $I_{ex} = 2$ and a ground-state spin $I_{gnd} = 0$. In the presence of a magnetic field, the excited state is split into five levels. For γ-ray propagation along the external field, this results in two transitions (corresponding to $\Delta I_z = \pm 1$) of equal intensity and separated in energy by $2g_n \mu_n H_n$, where H_n is the magnetic field at the nucleus. Ytterbium is divalent ($5f^{14}$), hence diamagnetic in the $TmAl_2$ source. One therefore has $H_n^{source} = H_{ext}$, and the emission spectrum consists of two lines separated by $2g_n\mu_n H_{ext}$. In $YbPd_3$, the ytterbium ion is trivalent and hence magnetic. The external field will then align the electronic moments and so produce a field H_{eff} at the nucleus. Thus one has $H_n^{abs} = H_{ext} + H_{eff}$, and the absorption spectrum consists of two lines with separation $2g_n\mu_n (H_{eff} + H_{ext})$. Since resonance occurs only between source and absorber lines having the same polarization, the resulting Mössbauer spectrum consists of two equally intense lines separated by $2g_n\mu_n H_{eff}$, with the external field not being seen explicitly. The electric quadrupole interaction will shift both lines by $-\frac{1}{8} e^2 q_{eff} Q$, where q_{eff} is the principal component of the electric-field-gradient tensor and Q is the quadrupole moment of the 2^+ state of ^{170}Yb.

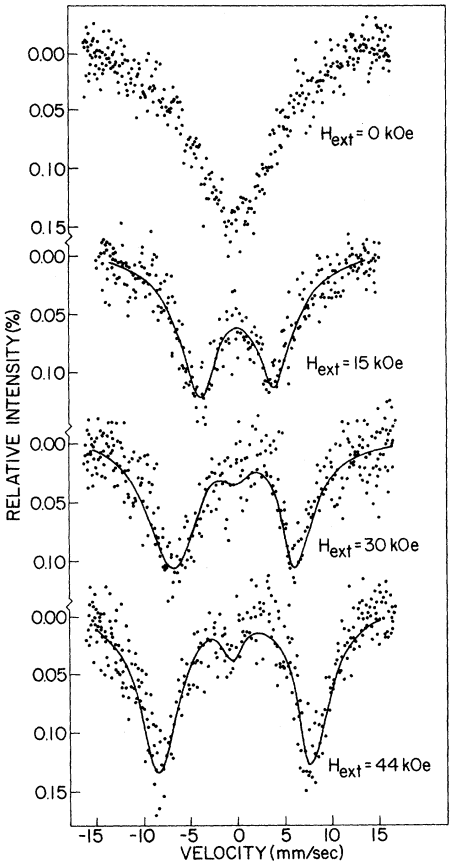

FIG. 1. Experimental hyperfine spectra for ^{170}Yb in $YbPd_3$ at $T = 4.2$ K.

Typical spectra are shown in Fig. 1. In low fields (≤ 5 kOe) one obtains a single broad line, with no structure resolved because of paramagnetic relaxation effects. In higher fields, the typical two line spectra are seen. These spectra were analyzed by a least-squares program to yield H_{eff} and q_{eff}. In the fitting procedure, finite intensity has been allowed for the $\Delta I_z = 0, \pm 2$ lines to allow for incomplete polarization due to a finite magnetic anisotropy. In addition, the lines are broadened because of distribution in H_{eff} and q_{eff} and because of effects of paramagnetic relaxation, as discussed below. These various effects combine to produce the asymmetric appearance of the spectra seen in Fig. 1. No evidence of magnetic ordering is seen down to 1.4 K.

Hyperfine Structure of Trivalent ^{170}Yb

Before discussing the experimental results it will be useful to consider in more detail the kinds of spectra that can be obtained under various conditions. In the absence of crystalline fields and external magnetic fields, all electronic levels of Yb^{3+} are degenerate and one obtains a "free-ion" hyperfine interaction

$$\mathcal{H}_{hf} = A_{fi} \vec{J} \cdot \vec{I} \tag{1}$$

with $A_{fi} = 1.03 \times 10^{-2}$ cm^{-1}. In a cubic crystalline field, the ground state of $Yb^{3+}(^2F_{7/2})$ splits into two doublets (Γ_6 and Γ_7) and one quartet (Γ_8), with wave functions as given in Table I.[5,6] These wavefunctions are independent of the crystalline field parameters, and one may therefore completely characterize the hyperfine spectra arising from each isolated level *a priori*. In this section we will describe the hyperfine results anticipated when any one of the levels (Γ_6, Γ_7, or Γ_8) is the ground state. These results apply only when the Zeeman interaction energy is small compared with the crystalline field energy, so that H_{ext} does not mix the different levels together.

1. *Doublets* Γ_6 *and* Γ_7

For both of the Kramers doublets Γ_6 and Γ_7, one can show from the wave functions in Table I that the quadrupole interaction is identically zero and that the states are isotropic ($g_x = g_y = g_z$). In the absence of external fields, the hyperfine interaction may then be described by a spin Hamiltonian of the form

$$\mathcal{H}_{hf} = A \vec{S} \cdot \vec{I} \quad , \tag{2}$$

with an effective spin $S = \frac{1}{2}$. The interaction constants are found to be $A(\Gamma_6) = -\frac{7}{3} A_{fi}$ and $A(\Gamma_7) = 3 A_{fi}$. If one defines a total angular momentum $\vec{F} = \vec{I} + \vec{S}$, then the eigenvalues of Eq. (2) are given by

$$E_F = \tfrac{1}{2} A[F(F+1) - I(I+1) - S(S+1)]. \tag{3}$$

In the present case ($I = 2$, $S = \frac{1}{2}$) we may have $F = \frac{3}{2}$ or $\frac{5}{2}$. Therefore the nuclear excited state will be split by the hyperfine interaction into two levels at energies $E_{5/2} = A$ and $E_{3/2} = -\frac{3}{2} A$. The ground state ($I = 0$) remains unsplit. For spin-relaxation times long compared to the Larmor precession time [i.e., for $(A/h)\tau_R \gg 1$], the Mössbauer spectrum will consist of lines located at positions $E_{5/2}$ and $E_{3/2}$ with relative intensities 3 and 2, respectively. For short relaxation times, a single line will be observed at zero energy. The zero-field data of Fig. 1 represents a case of intermediate

TABLE I. Electronic wave functions for a $^2F_{7/2}$ state in a cubic crystalline field. The components are labeled $|J_z\rangle$.

Γ_6:	$\sqrt{\frac{5}{12}}\,\lvert\pm\tfrac{7}{2}\rangle + \sqrt{\frac{7}{12}}\,\lvert\mp\tfrac{1}{2}\rangle$
Γ_7:	$\sqrt{\frac{3}{4}}\,\lvert\pm\tfrac{5}{2}\rangle - \sqrt{\frac{1}{4}}\,\lvert\mp\tfrac{3}{2}\rangle$
Γ_8:	$\sqrt{\frac{7}{12}}\,\lvert\pm\tfrac{7}{2}\rangle - \sqrt{\frac{5}{12}}\,\lvert\mp\tfrac{1}{2}\rangle$
	$\sqrt{\frac{1}{4}}\,\lvert\pm\tfrac{5}{2}\rangle + \sqrt{\frac{3}{4}}\,\lvert\mp\tfrac{3}{2}\rangle$

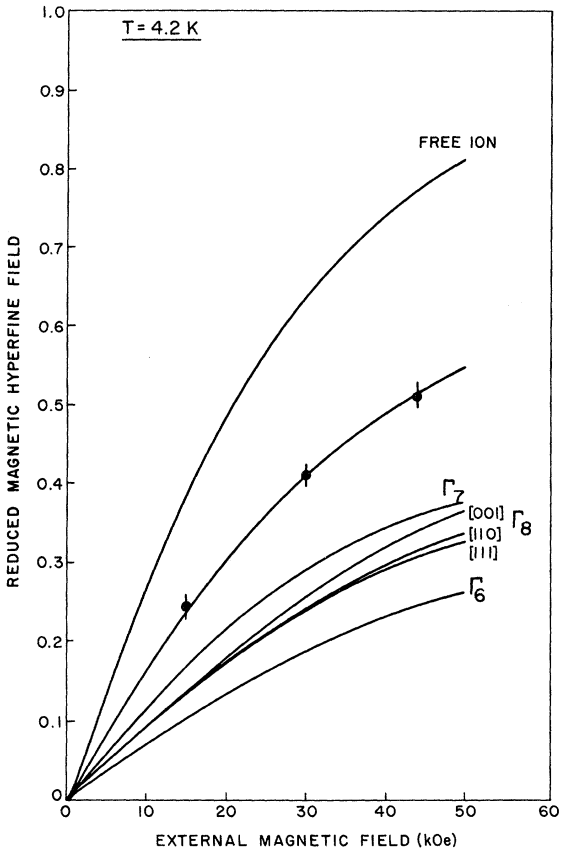

FIG. 2. Dependence of H_{eff} on H_{ext} at 4.2 K. Solid circles are experimental points. Solid line through data points is theoretical curve obtained as described in text with the values $A_4\langle r^4\rangle = -12$ cm^{-1} and $A_6\langle r^6\rangle = 0.6$ cm^{-1}. Other solid curves show the dependence expected if Γ_6, Γ_7, or Γ_8 is the ground state and no other level is mixed by the external field. For the case of Γ_8, three curves show the different dependences for H_{ext} along the three major symmetry axes. Also shown is the free-ion behavior.

relaxation times.

In an external magnetic field H_{ext}, the doublet degeneracy is removed by the Zeeman interaction $g\mu_B \vec{S}\cdot\vec{H}_{ext}$, where $g(\Gamma_6) = -\frac{8}{3}$ and $g(\Gamma_7) = \frac{24}{7}$. For external fields $H_{ext} \gg A/2g\mu_B \sim 1$ kOe, I and S are decoupled. Then the "effective-field approximation" is in effect and one has $\langle S_x\rangle = \langle S_y\rangle = 0$ with the z axis being along the direction of the external field. In the limit of fast spin relaxation, the external field aligns the electronic moment to produce an effective hyperfine field H_{eff} which depends on temperature and on H_{ext} according to

$$g_n\mu_n H_{eff} = \tfrac{1}{2}A \tanh(g\mu_B H_{ext}/2kT) \ . \qquad (4)$$

In the case of long spin-relaxation times, H_{eff} will be independent of H_{ext} and T and will have the saturation value $A/2g_n\mu_n$. The dependence of H_{eff} on H_{ext} from Eq. (4) is shown in Figs. 2 and 3 at temperatures of 4.2 and 1.4 K, respectively.

2. *Quartet* Γ_8

One easily verifies from the wave functions of Table I that the Γ_8 quartet is anisotropic and that the quadrupole interaction does not vanish. For $H_{ext} = 0$, the spin Hamiltonian is[5]

$$\mathcal{H}_{hf} = a\vec{I}\cdot\vec{S} + a'(I_xS_x^3 + I_yS_y^3 + I_zS_z^3) + b\sum_{q=x,y,z}[3I_q^2 - I(I+1)][3S_q^2 - S(S+1)] + b'\sum_{p\neq q}{}'(I_pI_q + I_qI_p)(S_pS_q + S_qS_p), \qquad (5)$$

where $S = \frac{3}{2}$. The constants a, a', b, and b' may be determined according to the procedures of Ref. 5. For the ^{170}Yb case, the combined electronic-nuclear state has a degeneracy of $(2I+1)(2S+1) = 20$ which is split by the hyperfine interaction into four doublets and three quartets.[7] Thus a seven line spectrum should be observed. However, in most cases the relaxation times are so short that this detailed structure is not seen.

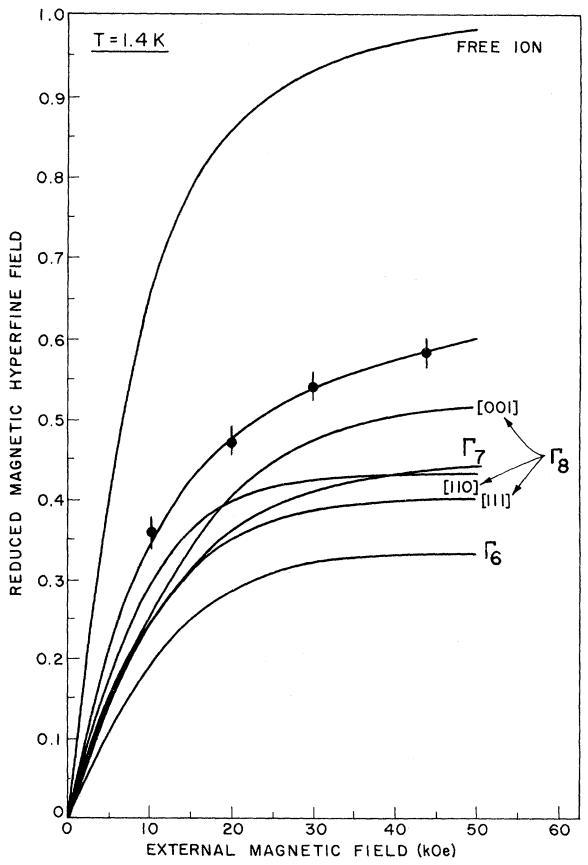

FIG. 3. Dependence of H_{eff} on H_{ext} at 1.4 K. Same details as in Fig. 2.

In the presence of an external field H_{ext}, the electronic wave functions are determined by the Zeeman interaction. In the spin formalism of the Γ_8 state, this must be written[5]

$$\mathcal{H}_{Zee} = g\mu_B \vec{S} \cdot \vec{H}_{ext} + f(H_x S_x^3 + H_y S_y^3 + H_z S_z^3), \quad (6)$$

where f is a known constant and the H_i are components of H_{ext} relative to the cube axes. This causes an anisotropic splitting of the Γ_8 state, and hence also an anisotropic hyperfine field. That is, the hyperfine field H_{eff} depends not only on the value of H_{ext}, but also on its orientation with respect to the crystalline axes. Nonetheless, for a given orientation the electronic wave functions may be obtained from Eq. (6) and H_{eff} (as well as q_{eff}) calculated. The dependence of H_{eff} on H_{ext} is shown in Figs. 2 and 3 at temperatures of 4.2 and 1.4 K for those cases in which the external field is along each of the three major symmetry axes [001], [110], or [111].

EXPERIMENTAL RESULTS AND DISCUSSION

Experimental values for the hyperfine field at various fields and at temperatures of 1.4 and 4.2 K are shown in Figs. 2 and 3. The experimental points do not follow any of the curves discussed above. Thus one concludes that the Zeeman interaction energy is comparable with the crystalline field splittings and that the ground state of Yb^{3+} in $YbPd_3$ in the presence of an external field is not an isolated level. In order to analyze the results we must solve the full Hamiltonian for an ion in a cubic crystal field and external magnetic field:

$$\mathcal{H} = A_4\langle r^4\rangle\langle J||\beta||J\rangle(O_4^0 + 5O_4^4) + A_6\langle r^6\rangle\langle J||\gamma||J\rangle(O_6^0 - 21\,O_6^4) - g_J\mu_B \vec{J}\cdot\vec{H}_{ext}. \quad (7)$$

The nonenclature of Eq. (7) is that of Lea, Leask, and Wolf.[6] Diagonalization of this Hamiltonian then yields electronic energy levels ϵ_i and wave functions ψ_i with which all observables can be calculated. For a given orientation of H_{ext} with respect to the crystalline axes, the effective magnetic hyperfine field $\vec{H}_{eff}$ and electric field gradient q_{eff} may thus be obtained. The magnetic hyperfine field is

$$\vec{H}_{eff}(H_{ext}, T) = H_{fi}\frac{\sum_i \langle\psi_i|\vec{J}|\psi_i\rangle e^{-\epsilon_i/kT}}{\sum_i J e^{-\epsilon_i/kT}} \equiv |H_{eff}|\,\hat{h}, \quad (8)$$

where $H_{fi} = 4230$ kOe is the free-ion hyperfine field and $\hat{h}$ is a unit vector. The components of the electric-field-gradient tensor q_m are given by

$$q_m(H_{ext}, T) = q_{fi}\frac{\sum_i \langle\psi_i|O_m^2|\psi_i\rangle e^{-\epsilon_i/kT}}{\sum_i J(2J-1)e^{-\epsilon_i/kT}}, \quad (9)$$

where $q_{fi} = -8.44\times10^{18}$ V/cm^2 is the free-ion value for the principal component and the O_m^2 are given by

$$O_0^2 = 3J_z^2 - J(J+1),$$
$$O_{\pm1}^2 = \mp\sqrt{\tfrac{3}{2}}[J_zJ_\pm + J_\pm J_z], \quad (10)$$
$$O_{\pm2}^2 = \sqrt{\tfrac{3}{2}}J_\pm^2.$$

For an electric quadrupole interaction small compared to the magnetic interaction, we may define an effective electric field gradient by projecting the components q_m along the direction of H_{eff}. This gives

$$q_{eff} = \tfrac{1}{2}q_0(3h_z^2 - 1) + \sqrt{\tfrac{3}{2}}(q_{+1}h_-h_z - q_{-1}h_+h_z) + \sqrt{\tfrac{3}{8}}(q_{+2}h_-^2 + q_{-2}h_+^2), \quad (11)$$

where $h_\pm = h_x \pm ih_y$, and $\hat{h}$ is defined in Eq. (8).

To obtain the parameters for a powder sample, one should then average over all orientations of H_{ext}. However the general calculation is quite tedious and complicated. To overcome these difficulties, we will assume that the anisotropy energy is low enough so that H_{eff} lies along the external field direction. If this were rigorously true, the spectra of Fig. 1 would consist of only two lines ($\Delta I_z = \pm1$). The experimental justification for the approximation thus lies in the fact that the $\Delta I_z = 0, \pm2$ transitions are observed with only very weak intensity. If in addition H_{ext} lies along one of the crystalline symmetry axes [001], [110], or [111], one can express the crystalline field in the coordinate system for which the direction of H_{ext} is the quantization axis.[8] Then, the hyperfine field and electric field gradient along the quantization axis will be given by

$$H_{eff}(T, H_{ext}) = \frac{H_{fi}\sum_i \langle\psi_i|J_z|\psi_i\rangle e^{-\epsilon_i/kT}}{\sum_i J e^{-\epsilon_i/kT}} \quad (12)$$

and

$$q_{eff}(T, H_{ext}) = \frac{q_{fi}}{J(2J-1)} \times \frac{\sum_i \langle\psi_i|3J_z^2 - J(J+1)|\psi_i\rangle e^{-\epsilon_i/kT}}{\sum_i e^{-\epsilon_i/kT}}. \quad (13)$$

We will evaluate these quantities and then approximate the average over direction by

$$\bar{H}_{eff} = \tfrac{1}{26}\{6H_{eff}([001]) + 8H_{eff}([111]) + 12H_{eff}([110])\}, \quad (14)$$

with a similar expression for $\bar{q}_{eff}$. The value for each direction is weighted according to the number of times that direction appears on the unit sphere. The results for a typical set of parameters shown in Table II. One sees that H_{eff} is not strongly dependent on orientation, whereas q_{eff} varies a large amount. We thus expect little error in the average

TABLE II. Calculated values of hyperfine constants showing the anisotropy in H_{eff} and q_{eff} for $H_{ext}=40$ kOe and $T=1.4$ K. The crystal field parameters $A_4\langle r^4\rangle = -12$ cm^{-1} and $A_6\langle r^6\rangle = 0.6$ cm^{-1} used are those which best describe the experimental results.

Axis	H_{eff}/H_{fi}	q_{eff}/q_{fi}
[110]	0.589	0.181
[111]	0.549	0.179
[100]	0.528	0.050
Average according to Eq. (14)	0.562	0.150

H_{eff} due to the approximation of Eq. (14), whereas the average q_{eff} obtained in this way must not be relied on.

In summary, our procedure has been to diagonalize the general Hamiltonian for the three major directions, calculate $\bar{H}_{eff}(H_{ext}, T)$ and $\bar{q}_{eff}(H_{ext}, T)$ as above for various values of the crystal field parameters A_4 and A_6, and compare the results with the data. The solid lines through the data points of Figs. 2 and 3 are the best fit, obtained for values $A_4\langle r^4\rangle = -12\pm 1$ cm^{-1} and $A_6\langle r^6\rangle = 0.6 \pm 0.6$ cm^{-1}. Values of $\bar{q}_{eff}$ calculated with these parameters show generally good agreement with the experimentally observed dependence on H_{ext} and T. However the quadrupole interaction is rather small, hence the experimental errors are large. This coupled with the large directional dependence of the calculated q_{eff} makes a detailed comparison difficult.

These values for the crystal field constants imply that Yb^{3+} in $YbPd_3$ has a Γ_7 ground state with Γ_8 and Γ_6 lying at approximately 29 and 39 cm^{-1}, respectively. This is roughly one order of magnitude lower than is observed in cubic Yb^{3+} insulators. For example, Yb^{3+} in CaF_2 has the Γ_7 level as ground state,[9] with Γ_8 lying at 604 cm^{-1}. These crystal field parameters, when extrapolated to other similar compounds, verify previous suggestions[10] that the magnetic Γ_5 state is the ground level for Pr^{3+} in $PrPd_3$ and that the Γ_8 level is the ground state for Sm^{3+} in $SmPd_3$. More specifically, we may estimate $A_4\langle r^4\rangle$ for Sm^{3+} by multiplying the experimental value obtained for Yb^{3+} by the ratio $\langle r^4\rangle_{Sm^{3+}}/\langle r^4\rangle_{Yb^{3+}}$ given by Hartree-Fock calculations.[11] The resulting values of $A_4\langle r^4\rangle_{Sm^{3+}} = 22$ cm^{-1}, $A_6\langle r^6\rangle \simeq 0$, when combined with the calculations of Lea, Leask, and Wolf, give a separation of 30 K between the Γ_8 and Γ_7 levels in $SmPd_3$. This is in sufficient agreement with the crude estimate of 100 K obtained from magnetic susceptibility data.[10]

It is of interest to compare the measured crystalline field parameters with predictions of a simple point-charge model. If a is the unit cell dimension, then in $YbPd_3$ (Cu_3Au structure) the Yb^{3+} ion has 12 Pd first neighbors at distances of $a/\sqrt{2}$, six Yb second-nearest neighbors at distances a, and 12 Yb third-nearest-neighbors at distances $a\sqrt{2}$. These give crystal field constants

$$A_4\langle r^4\rangle = (e^2\langle r^4\rangle/a^5)(\tfrac{7}{8}\sqrt{2}\ Z_1 - \tfrac{7}{16}\ Z_2 + \tfrac{7}{256}\sqrt{2}\ Z_3),$$
$$A_6\langle r^6\rangle = (e^2\langle r^6\rangle/a^7)(\tfrac{32}{39}\sqrt{2}\ Z_1 - \tfrac{3}{64}\ Z_2 + \tfrac{1}{156}\sqrt{2}\ Z_3), \quad (15)$$

where Z_1, Z_2, and Z_3 are the charges which the Yb ion sees on the first, second, and third neighbors, respectively. The third neighbor contributes only ~10% to $A_4\langle r^4\rangle$ even if we use the full unshielded values $Z_3 = Z_2$, and so will be neglected. With the values $a=4.0317$ Å (Ref. 4), $\langle r^4\rangle = 0.96$ a.u., and $\langle r^6\rangle = 3.104$ a.u. (Ref. 11), we obtain

$$A_4\langle r^4\rangle = 10.1\,[Z_1 - (Z_2/2.83)]\ \text{cm}^{-1},$$
$$A_6\langle r^6\rangle = 0.8\,[Z_1 - (Z_2/36.77)]\ \text{cm}^{-1}. \quad (16)$$

If Z_1 is positive, and we assume Z_2 small because of screening effects, then the calculated and measured A_4 values disagree in sign. The only possible agreement with the nearest-neighbor-only approach comes from an assumption of $Z_1 = -1$, which does not seem likely in these metallic systems. On the other hand, if we assume $Z_1 \sim 0$, then the sign disagreement is not present. We may justify this with the observation that the compounds YPd_3, $LaPd_3$, and $LuPd_3$ are all diamagnetic.[10,12] With the exception of $EuPd_3$ and $SmPd_3$, the paramagnetic moment for all the other $R\,Pd_3$ (R = rare earth) compounds agree with the R^{3+} free-ion value.[10,12] Thus the Pd carries no magnetic moment in these systems, hence must have a closed d shell, and the neutral atom configuration of $4d^{10}$ seems

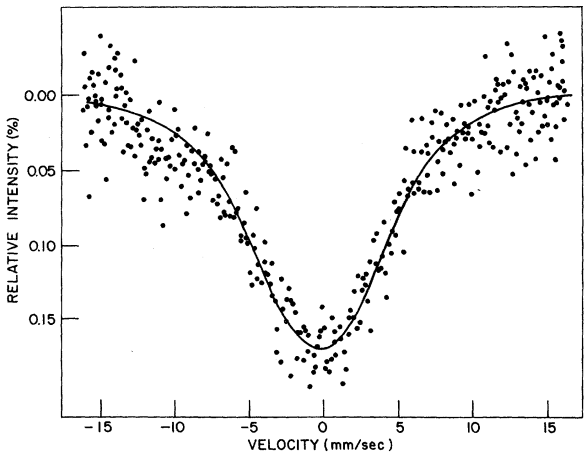

FIG. 4. Hyperfine spectrum for $H_{ext}=5$ kOe and $T=4.2$ K. Solid line is calculated allowing paramagnetic relaxation with a spin-relaxation time $\tau_R \sim 4\times 10^{-11}$ sec.

reasonable.[13] In fact, with $Z_1 = 0$ for a neutral Pd atom and with $Z_2 = 3$ for an unscreened Yb^{3+} ion, one finds from the above $A_4\langle r^4\rangle = -10.7$ cm^{-1} and $A_6\langle r^6\rangle = -0.06$ cm^{-1}. Such excellent agreement with experiment is probably coincidental. However, in most cases one finds that such simple calculations will reproduce the order of magnitude and the correct sign for the crystal field parameters,[14] and the present result is in line with that general feature. It may also be noted that simple nearest-neighbor calculations have recently been very successful in calculating crystal field parameters for a number of rare-earth metallic compounds.[1] The apparent success of what seems to be a naive model is not understood. In view of the present agreement with experiment, we have made no attempt to interpret the data in terms of more sophisticated approaches, such as in Ref. 2.

In low-field spectra ($H_{ext} \leq 5$ kOe) only one very broad line is observed. Assuming that the broadening is due to slow spin relaxation processes, we have analyzed the spectra with the simple two-level relaxation expression[15] appropriate for an isolated Kramers doublet, since 5 kOe is insufficient to mix an appreciable fraction of the Γ_8 level. An example is given in Fig. 4. This analysis provides an electronic spin-relaxation time $\tau_R \simeq 4 \times 10^{-11}$ sec, roughly independent of H_{ext} and T. These spectra were analyzed assuming complete polarization, i.e., that the intensity of the $\Delta I_z = 0, \pm 2$ lines was zero. Attempts to fit with a full five line spectra were quite unsuccessful. This indicates that the observed magnetic anisotropy at higher fields is due solely to the anisotropy of the Γ_8 level which is admixed into the ground state by the applied field. This is also indicated by the increase in the intensity of the $\Delta I_z = 0$ transition as the external field is increased (see Fig. 1).

†Based on work performed under the auspices of the U. S. Atomic Energy Commission.

*On leave from the Hebrew University, Jerusalem, Israel.

‡Permanent address: Physik Department, Technische Universität München, D8000 Munich, West Germany.

[1]K. C. Turberfield, L. Passel, R. J. Birgeneau, and E. Bucher, Phys. Rev. Letters 25, 752 (1970); J. Appl. Phys. 42, 1746 (1971).

[2]G. Williams and L. L. Hirst, Phys. Rev. 185, 407 (1969).

[3]D. Davidov, R. Orbach, C. Rettori, D. Shaltiel, L. J. Tao, and B. Ricks, Phys. Letters 37A, 361 (1971); 35A, 339 (1971).

[4]I. R. Harris and G. V. Raynor, J. Less-Common Metals 9, 263 (1965).

[5]A. Abragam and B. Bleaney, *Electron Paramagnetic Resonance of Transition Ions* (Clarendon, Oxford, 1970), pp. 721–732.

[6]K. R. Lea, H. J. M. Leask, and W. P. Wolf, J. Phys. Chem. Solids 23, 1381 (1962).

[7]H. Eicher, Z. Physik 169, 178 (1962).

[8]M. T. Hutchings, Solid State Phys. 16, 277 (1966).

[9]J. M. Baker, W. B. J. Blake, and G. M. Copland, Proc. Roy. Soc. (London) A309, 119 (1969).

[10]W. E. Gardner, J. Denfold, and I. R. Harris, J. Phys. (Paris) 32, (1971).

[11]A. J. Freeman and R. E. Watson, Phys. Rev. 127, 2058 (1962).

[12]R. D. Hutchens, V. U. S. Rao, J. E. Greedau, W. E. Wallace, and R. S. Craig, J. Appl. Phys. 42, 1293 (1971).

[13]A similar argument has been used for the rare-earth–Ni_2 system by B. Bleaney, Proc. Roy. Soc. (London) 276, 28 (1963).

[14]For a notable exception, see Ref. 2.

[15]I. Nowik and H. H. Wickman, Phys. Rev. Letters 17, 949 (1966).

PHYSICAL REVIEW B VOLUME 6, NUMBER 3 1 AUGUST 1972

Spin-Wave Approach to One-Dimensional Antiferromagnetic $CsNiCl_3$ and $RbNiCl_3$

P. A. Montano, E. Cohen, and H. Shechter
Department of Physics, Technion, Israel Institute of Technology, Haifa, Israel
(Received 7 February 1972)

The spin-wave approximation is applied to linear-chain antiferromagnets $CsNiCl_3$ and $RbNiCl_3$. The susceptibility as well as the zero-temperature magnetic moment is calculated. There is good agreement between the experimental results and the theoretical calculations.

Recently attention has been focused on substances that exhibit one-dimensional properties,[1] such as $CsNiCl_3$ and $RbNiCl_3$. These have chains of octahedrally coordinated Ni^{2+} ions along the c axis. At low temperatures and above their three-dimensional ordering temperatures (11 and 4.5 °K for $RbNiCl_3$ and $CsNiCl_3$, respectively) these compounds show many of the characteristics of linear antiferromagnets.[2] A very interesting result has been obtained by Cox and Minkiewicz.[3] They showed that the magnitude of the Ni^{2+} moment in $CsNiCl_3$ extrapolated to 0 °K is $(1.05 \pm 0.1)\mu_B$ (μ_B is the Bohr magneton). They attributed it to a very substantial zero-point deviation. In this paper we re-